AIAA JOURNAL
Vol. 32, No. 12, December 1994

Active Boundary-Layer Control in Diffusers

Anthony H. M. Kwong* and Ann P. Dowling†
Cambridge University, Cambridge CB2 1PZ, England, United Kingdom

Flow separation in diffusers leads to loss in energy recovery and is often a source of unsteadiness due to stall movements. This paper investigates the use of wall jets as a remedy to these problems. New jet geometries are compared to the conventional annular blowing. Steady wall jets are found to be capable of raising the mean pressure recovery in both conical and rectangular air diffusers, but high injected mass flow rates are required before the flow in rectangular diffusers becomes steady. Active feedback control is applied to reduce this flow unsteadiness. To implement the control, the air supplied through the wall jets is modulated in response to the unsteady pressures within the diffuser. Results are presented for two feedback mechanisms. Both are found to be effective with the level of attenuation well predicted by theory. A combination of steady and unsteady blowing is found to be capable of giving both a good mean pressure recovery and reduced pressure oscillations.

Nomenclature

A_d = diffuser inlet area
A_j = wall jet exit area
A_2 = diffuser exit area
$\bar{C}_p$ = diffuser recovery coefficient
D = conical diffuser inlet diameter
d = orifice diameter
L = axial diffuser length
Ma = Mach number
$\bar{m}_d$ = mean diffuser mass flow rate
$\bar{m}_j$ = mean wall jet mass flow rate
p_1 = diffuser inlet gauge pressure
p_2 = diffuser exit gauge pressure
Re_l = Reynolds number based on length l
s = Laplace transform variable
$\bar{u}_d$ = mean diffuser inlet flow velocity
$\bar{u}_j$ = mean wall jet exit flow velocity
W_1 = rectangular diffuser inlet width
Δp = diffuser recovery pressure, $p_2 - p_1$
ρ = fluid density

I. Introduction

A DIFFUSER aims to slow down a mean flow, converting its kinetic energy into a pressure rise. At all but the smallest diffuser divergence angles, this adverse pressure gradient causes flow separation, with an appreciable reversed flow in the diffuser. The pressure recovery is then far less than its ideal or inviscid value. The flow is highly unsteady in rectangular diffusers[1] with divergence angles that give a high mean pressure recovery, a phenomenon which is commonly referred to as transitory stall.[2]

Different devices for separation control have been reported in the past. A thorough review can be found in Gad-el-Hak and Bushnell.[3] Among those a particularly successful technique is the injection of high momentum fluid into the separating boundary layers. In diffusers, this can delay separation and increase the pressure recovery. Most of the previous work on wall jets has been concerned with annular injection into conical diffusers. Nicoll and Ramaprian[4] redefined the pressure recovery coefficient to account for the injection energy. Even so, they found that optimal blowing with a tangential annular wall jet in a conventional conical diffuser could increase the value of the pressure recovery coefficient by about 70%. Later Duggins[5] and Duggins et al.[6] published two sets of results and concluded that an axial annular wall jet is better than one tangential to the wall. By varying the annular jet height, it was discovered that diffuser performance with steady blowing is governed primarily by the momentum of the injected fluid. Reports of the effects of wall jets in rectangular diffusers are relatively scarce. Tangential blowing with slot jets was examined by Fiedler and Gessner.[7] Despite their conclusion that an improvement in effective performance had been obtained and might exceed those realizable by other boundary-layer control methods, differences in their definition of the recovery coefficient make comparison with the conical cases impossible.

Transitory stall induces flow fluctuations. These can easily couple with other flow devices to give large flow unsteadiness.[8] Smith[9] suggested that unsteady diffuser behavior may play a major role in initiating centrifugal compressor stage stall. Moreover, diffusers are often used to slow down a fluid flow prior to combustion and can couple to combustion oscillations resulting in significant pressure oscillations.[10]

In this paper, steady wall jets of various geometries in conical and rectangular diffusers are investigated. We find that a distribution of circular nozzles can achieve a similar optimal pressure recovery coefficient to an annular jet, with only about half of the rate of mass injection. Active control methods[11] have been used extensively to reduce flow unsteadiness.[12] We investigate their effectiveness at reducing oscillations due to transitory stall. The control is implemented by modulating the air supplied through the wall jets in response to the unsteady pressures within the diffuser. A combination of steady and unsteady blowing is shown to be capable of giving both a good mean pressure recovery and reduced pressure oscillations.

II. Steady Blowing in a Conical Diffuser

A $2\theta = 16$-deg, $L/D = 8$, $D = 95$-mm conical air diffuser is used. According to McDonald and Fox's performance maps,[13] the flow in such a diffuser is classified as exhibiting fixed-intermittent-transitory stall. Upstream of the diffuser, ambient air enters a 400-mm straight inlet pipe through a bell mouth. A trip ring of height 2 mm is located in the inlet pipe to produce a turbulent boundary layer and an area blockage of 15% at the diffuser inlet. The diffuser exhausts into a $1.82 \times 1.21 \times 1.21$-m^3 plenum chamber, which is connected to a variable speed axial blower. The geometry is illustrated in Fig. 1.

Pressure measurements are made by Druck PDCR 800 pressure transducers (range ± 70 mbar with a corresponding output of ± 17 mV). The first stage of amplification uses a low noise OP-27G operational amplifier by Analog Devices. The transducers are connected to the diffuser and the inlet pipe through plastic hoses and tappings of diameter 2.5-mm mounted flush in the walls. At frequencies of interest (less than 10 Hz), attenuation and phase errors

Presented as Paper 93–3255 at the AIAA 3rd Shear Flow Control Conference, Orlando, FL, July 6–9, 1993; received Sept. 27, 1993; revision received June 16, 1994; accepted for publication June 20, 1994.

*Research Student, Engineering Department, Trumpington Street; currently Research Officer at EDC, School of Mechanical Engineering, University of Bath, Claverton Don Bath BA2 7AY. Member AIAA.

†Professor, Engineering Department, Trumpington Street. Member AIAA.

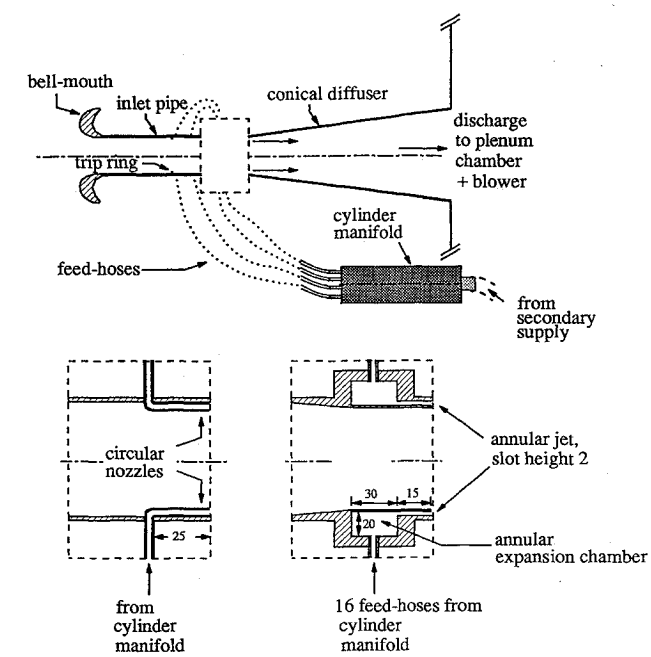

Fig. 1 Schematic diagram of jet systems.

induced by these connections are negligible in theory.[14] The pressure p_1 is measured on the straight inlet pipe immediately upstream of the sloping wall, whereas p_2 is measured on the sloping wall just before flow is discharged into the plenum chamber. Δp is measured directly by a pressure transducer connected across these two positions. The transducer accuracy, as calibrated by the manufacturer (< 0.06% full scale), leads to errors of less than ±1% within our data range.

Mean diffuser volume flow rate and inlet velocity may be deduced from the mean static pressure p_i measured at one inlet diameter D downstream of the intake end of the straight inlet section. Here the area blockage is found by hot-wire measurements to be less than 0.5%. By assuming an inviscid uniform flow at this section, the mean dynamic head can be equated to the mean gauge pressure p_i. Including the uncertainties in pressure measurement, this gives a maximum total error of ±3% in time-averaged inlet velocity and volume flow rate measurements.

Time histories and time-averaged measurements are made by feeding the preamplified transducer signals to a 12-bit Microlink data acquisition system. A 80-Hz cutoff low-pass antialiasing analogue filter is used for each logging channel at the sampling rate of 200 Hz. The maximum error due to quantization is 0.5%. Spectral data is collected by a Hewlett-Packard 5420B digital signal analyzer.

Steady blowing in three different configurations of wall jets is investigated. Secondary air is fed from an external supply; the flow rate being regulated by a proportional control valve. The first jet configuration involves eight circular nozzles of external and internal diameters 7 mm and 5 mm, respectively, distributed uniformly around the circumference at the diffuser inlet. The second system uses identical nozzles but increases the number to 16. The third one uses an annular jet as in Refs. 5 and 6 with a fixed slot height of 2 mm. Schematic diagrams of the circular nozzles and annular jet configuration are shown in Fig. 1.

The secondary air flow rate is measured by an orifice plate in its supply pipeline. The orifice plate was constructed according to the guidelines laid down by the British Standard Institution,[15] and so its flow coefficient is known to within ±2%. The pressure drop across the orifice is measured by a Sensym LX1804DZ pressure transducer. This leads to a maximum error of ±3% in determining $\bar{u}_j$, the time and area-averaged jet exit velocity.

Care was taken to ensure that the secondary flow is uniformly distributed between the circular nozzles. First, measurements confirmed that there is negligible pressure variation around the diffuser circumference in the nozzles' exit plane. Each nozzle is supplied

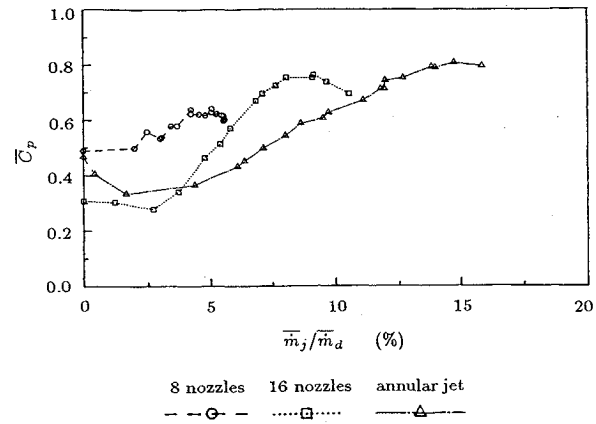

Fig. 2 Comparison of wall jet performance in conical diffuser.

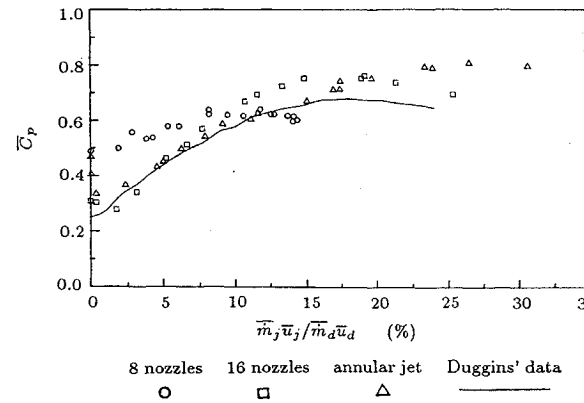

Fig. 3 $\bar{C}_p$ vs injected-to-diffuser momentum flux ratio.

through identical feed hoses of length 0.8 m and internal diameter 5 mm, connected to a cylindrical manifold of much larger cross-sectional area (diameter 75 mm, length 210 mm), as shown in Fig. 1. This serves to equalize the stagnation pressure of the air entering the feed hoses.

For the case of annular injection, an annular expansion chamber, whose cross-sectional area is 10 times that of the annular jet, is used to produce a jet flow with negligible circumferential variation (see Fig. 1).

Since external energy is fed into the diffuser, the following definition of the pressure recovery coefficient[4] $\bar{C}_p$, is used to account for the secondary injection energy:

$$\bar{C}_p = \frac{(\bar{m}_d + \bar{m}_j)\overline{\Delta p}}{\bar{m}_d \times \frac{1}{2}\rho\bar{u}_d^2 + \bar{m}_j \times \frac{1}{2}\rho\bar{u}_j^2}. \tag{1}$$

With $Re_D \simeq 3 \times 10^5$ ($\bar{u}_d \simeq 47$ m/s), $\bar{C}_p$ is plotted against the percentage injected-to-diffuser flow rate in Fig. 2. Significant variation is seen between the performance of the three injection systems. Practical interest is in the highest pressure recovery coefficient $\bar{C}_p$ that can be achieved. Injection through 8 nozzles can, at best, only produce a pressure recovery coefficient of 0.64. But both the 16 nozzles and the annular jet are effective ways of improving diffuser performance. The maximal values of $\bar{C}_p$ are 0.77 for 16 nozzles at $\bar{m}_j/\bar{m}_d \simeq 7.0\%$ and 0.81 for the annular jet at $\bar{m}_j/\bar{m}_d \simeq 14.0\%$.

In Duggins et al.[6] it is mentioned that the major disadvantages of using an annular wall jet are the complexity of the injection slot geometry and the need for an adequate supply of secondary fluid. It is evident from our results that by replacing an annular jet with 16 nozzles, the optimal recovery is reduced by just 5% whereas the required injection mass flow rate is halved. Moreover, the nozzles are considerably simpler to manufacture than an annular slit.

In Fig. 3, $\bar{C}_p$ is plotted against injected-to-diffuser momentum flux and the Duggins et al. data[6] from annular jets of different slot sizes are included for comparison. At low injection rates, the variation in $\bar{C}_p$ for the different injection systems is due to the different blockages they produce at the diffuser inlet. At moderate and high

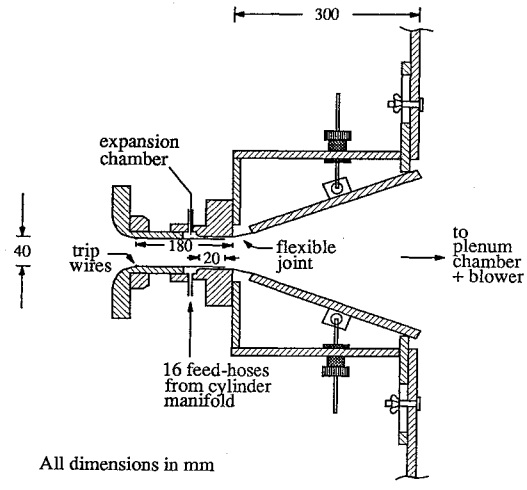

Fig. 4 Rectangular diffuser rig geometries.

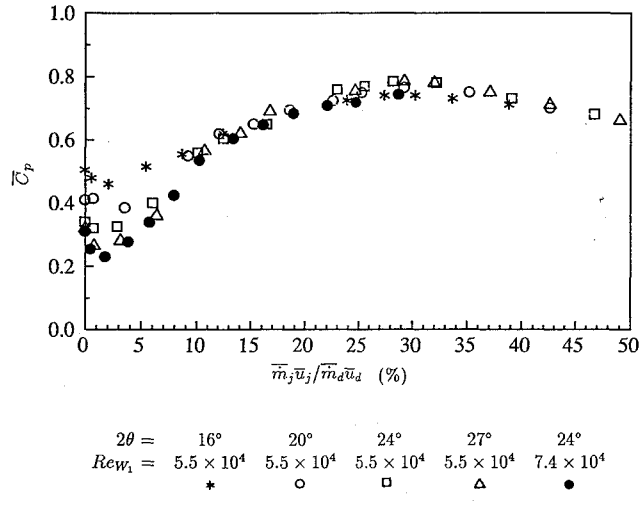

Fig. 5 Slot jet performance in rectangular diffuser.

injection rates, $\bar{m}_j\bar{u}_j/\bar{m}_d\bar{u}_d \geq 0.08$, much of the variation between the different injection systems evident in Fig. 2 is eliminated when injected-to-diffuser momentum flux is used as the independent variable. This agrees with Duggins' observation[5] that the $\bar{C}_p$ curves for annular jets of different slot heights collapse onto one another when plotted against injected-to-diffuser momentum flux. He concluded that diffuser performance is governed primarily by the momentum of the injected fluid. Here we see that the same conclusion remains approximately true even for different wall jet geometries. Since we have demonstrated that performance with steady blowing is more a function of the injected-to-diffuser momentum flux than the mass injection ratio, it may be argued that the optimum mass injection rate for an annular jet could be reduced by reducing the slot height. However, such slot heights are unrealistically small.

III. Steady Blowing in Rectangular Diffusers

A rectangular air diffuser, with $L/W_1 = 7.5$, $W_1 = 40$ mm, and aspect ratio 4.0, was used to investigate the effect of steady wall jets. Four trip wires of diameter 0.25 mm are placed around the perimeter just downstream of the bell mouth to ensure a turbulent boundary layer with an area blockage of 2% at diffuser inlet. The instrumentation is the same as that described for the conical diffusers, mean inlet velocity now being determined from a static pressure measured one inlet width W_1 downstream of the intake end of the straight inlet section. The inclined walls of the diffuser are attached to the straight inlet of length 180 mm through a flexible joint, allowing the wall angle θ on either side to vary from 0 to 20 deg, nonetheless keeping a smooth entrance profile.

Secondary air is injected axially on all four walls around the perimeter of the diffuser inlet, through a slot of height 2 mm ($A_j/A_d = 0.12$), as shown in Fig. 4. $\bar{C}_p$, as defined in Eq. (1), is plotted in Fig. 5 for symmetric diffuser settings of 2θ from 16 to 27 deg and two values of Re_{W_1}. The axial blowing starts to improve the pressure recovery coefficient when $\bar{m}_j\bar{u}_j/\bar{m}_d\bar{u}_d$ exceeds about 10% ($\bar{m}_j/\bar{m}_d > 10.9\%$). Thereafter, the five sets of data collapse onto a single curve reaching an optimal $\bar{C}_p$ of 0.78 at $\bar{m}_j\bar{u}_j/\bar{m}_d\bar{u}_d = 29\%$ ($\bar{m}_j/\bar{m}_d \simeq 18.7\%$). This curve coincides with that for the conical diffuser in Fig. 3.

IV. Spectral Analysis with Steady Blowing

As well as altering the mean recovery, axial blowing also affects the flow unsteadiness. The power spectral density of pressure fluctuations in the rectangular diffuser has been investigated for the combinations of diffuser divergence angles and Reynolds numbers shown in Fig. 5. All of the five sets of data follow the same general trend. A typical set of plots for Δp is given in Fig. 6 with $2\theta = 24$ deg and $Re_{W_1} \simeq 5.5 \times 10^4$ ($\bar{u}_d \simeq 21$ m/s).

Without any blowing, transitory stall unsteadiness occurs in this diffuser at frequencies less than 10 Hz. As pointed out by Kwong and Dowling,[8] flow visualizations and pressure measurements show that these fluctuations arise basically from two unsteady phenomena.

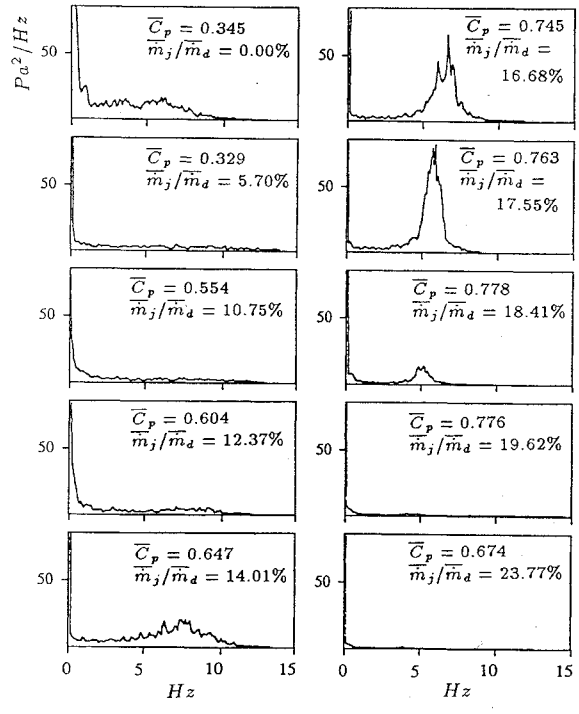

Fig. 6 Change in Δp spectrum with steady blowing.

The first is a low frequency (< 2 Hz) and highly random global switching of the stall from one diffuser corner to another. The second is a pseudoperiodic movement of the upstream edge of the stall cell. This latter phenomenon leads to the unsteadiness in the range 2–10 Hz.

When blowing is applied, even modest levels of injection ($\bar{m}_j/\bar{m}_d > 5\%$) are found to eliminate the low-frequency unsteadiness (< 2 Hz). This is confirmed by flow visualization which shows that the switching of the stall cell from one diffuser corner to another is suppressed by these levels of axial blowing. The higher frequency oscillations (2–10 Hz) are seen to reduce for blowing rates up to about 12%. After that, an increase in $\bar{m}_j/\bar{m}_d$ leads to a rise in unsteadiness with a well-defined spectral peak. As $\bar{m}_j/\bar{m}_d$ is increased further from 14 to 18%, the peak is observed to become stronger and narrower in bandwidth, while at the same time migrating toward a lower frequency. When the optimal blowing rate of 18.5% is reached, the peak starts to diminish, and increasing $\bar{m}_j/\bar{m}_d$ thereafter brings the flow back to a steady state.

V. Active Control with Zero Mean Blowing

With zero mean injection, a feedback system is used to reduce transitory stall unsteadiness in the rectangular diffuser. This arrange-

ment involves using a pressure transducer to monitor the flow perturbations in the diffuser and then driving an unsteady flow through the slot at the diffuser inlet in response to these fluctuations. We choose to use a loudspeaker as our actuator. It is sealed onto one side of an airtight container which is connected to the slot at the diffuser inlet. At these low frequencies, movements of the loudspeaker cone provide successive axial blowing and suction through the slot. This unsteady flow directly affects the inlet boundary layer to which the stall is particularly sensitive. In the last section, we mentioned that there are two modes of transitory stall unsteadiness. The first is a highly broadbanded global switching from one diffuser corner to another. Since this experiment aims at stabilizing the second mode of oscillation, the upstream edge transient behavior of the stall, the inlet unsteady pressure p_1 is chosen as the control objective. This avoids the broadbanded low-frequency signal (<2 Hz) in Δp, allowing the use of a simple feedback system.

At $2\theta = 24$ deg, $Re_{W_1} = 6.3 \times 10^4$ ($\bar{u}_d = 23.6$ m/s), the transfer function $G(s)$ between p_1 and the loudspeaker input voltage v_f is identified by sinusoidal forcing (Fig. 7). We seek to model this open-loop transfer function analytically. The transfer function must have at least two zeros to account for the rise in magnitude of about 30 dB/decade at low frequencies (< 8 Hz). The rapid decay at higher frequencies indicates that there should be five more poles than zeros. We, therefore, seek to model $G(s)$ by a function with two zeros and seven poles, the coefficients being determined by least-square-error minimization. The model generated by this system identification is compared with the experimental data in Fig. 7. It is clear that it matches the measurements well.

The response of the diffuser to noise can be represented by the block diagram in Fig. 8a. Here $n(s)$ is the system noise source. It may, for example, represent local turbulent fluctuations. $G_1(s)$, $G_2(s)$, and $G_3(s)$ are transfer functions describing the unsteadiness in p_1 due to $n(s)$ and $v_f(s)$. From Fig. 8a, we have

$$p_1(s) = [v_f(s)G_1(s) + n(s)G_3(s)]G_2(s) \tag{2}$$

The product $G_1(s)G_2(s)$ is the transfer function $G(s)$ shown in Fig. 7.

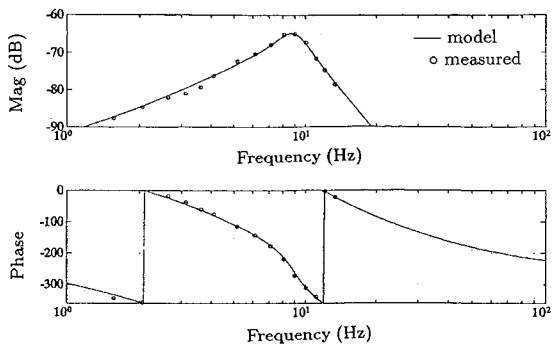

Fig. 7 System identification of $G(s)$ by sinusoidal forcing with loudspeaker.

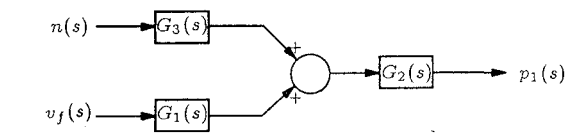

a) Without feedback

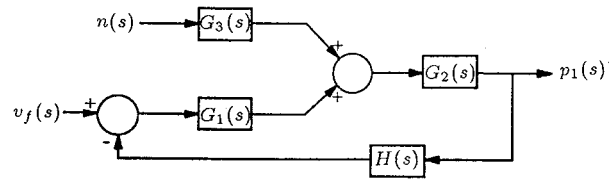

b) With feedback

Fig. 8 System block diagrams.

The block diagram for the system with active control is shown in Fig. 8b. Here the control signal $p_1(s)$ is fed back to drive the loudspeaker; $H(s)$ being the negative feedback filter. The system response to noise is determined by putting $v_f(s) = 0$ and is modified by feedback to

$$p_1(s) = \frac{n(s)G_2(s)G_3(s)}{1 + G_1(s)G_2(s)H(s)} \tag{3}$$

It is evident that, to reduce the system sensitivity to noise, we wish to make $|1+G_1(s)G_2(s)H(s)|$ as large as possible at all frequencies while, of course, keeping the system poles stable. Analysis of the Bode diagram in Fig. 7 suggests that a simple constant gain feedback is sufficient. The power spectra without and with control are plotted in Fig. 9 for $H(s) = 1500$. Active control reduces the spectrum peak at around 7 Hz by 7 dB and the total spectrum power by 20%. Nevertheless, the mean pressure recovery $\bar{C}_p = 0.36$ is measured to be unaltered by the feedback.

Figure 10 shows the measured attenuation as a function of frequency. If the noise source is unchanged by the feedback, it is evident from a comparison of Eqs. (2) and (3) that for $v_f(s) = 0$ (i.e., no external forcing of the loudspeaker),

$$\frac{p_1(j\omega)|_{\text{with control}}}{p_1(j\omega)|_{\text{without control}}} = \frac{1}{1 + G_1(j\omega)G_2(j\omega)H(j\omega)} \tag{4}$$

This theoretical attenuation is compared with the measured one in Fig. 10. Good agreement is found, confirming our assumption that the noise source is uninfluenced by the feedback. Consequently, the modification in global pressure p_1 does not alter the noise source. This implies that the source of disturbance forcing the unsteady diffuser flow is likely to be a local quantity like, for example, turbulent eddies in the boundary layers.

VI. Active Control Around Optimal Blowing

We mentioned in Sec. IV the presence of some strong unsteadiness with near-optimal steady blowing. A second control system,

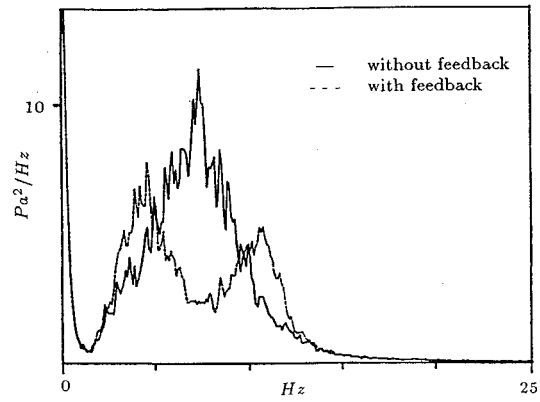

Fig. 9 Effect of active control with zero mean blowing rate.

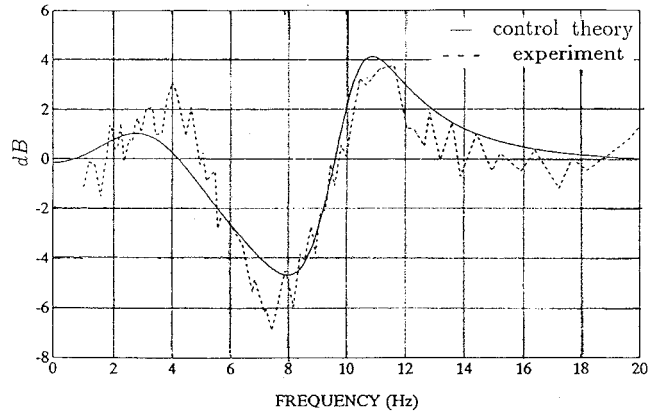

Fig. 10 Comparison of measured attenuation with theory, $\bar{m}_j/\bar{m}_d = 0\%$.

therefore, is developed to be implemented with steady blowing to ensure both good pressure recovery and stable dynamic response. At $2\theta = 24$ deg and $Re_{W_1} = 5.5 \times 10^4$ ($\bar{u}_d = 20.6$ m/s), feedback is realized by adding an unsteady signal to the proportional control valve input which in turn regulates the rate of injection unsteadily, while keeping the mean flow rate ratio $\bar{m}_j/\bar{m}_d$ constant. With this rate of blowing, the highly random stall switch phenomenon is eliminated (see Fig. 6). As a result, Δp is taken as the control objective which is, perhaps, more representative of diffuser unsteadiness.

System identification procedures described for feedback with the loudspeaker are repeated. The Bode diagram from sinusoidal forcing of the proportional control valve is shown in Fig. 11. The amplitude drop of about 60 dB/decade at high frequencies and the flat response at low frequencies suggest that we model this open-loop behavior by an analytical function with three poles and no zeros. To account for the delayed response in the proportional control valve (i.e., the dead time), this third-order transfer function is multiplied by a time delay term $e^{-s\tau}$ before least square fitting is applied.

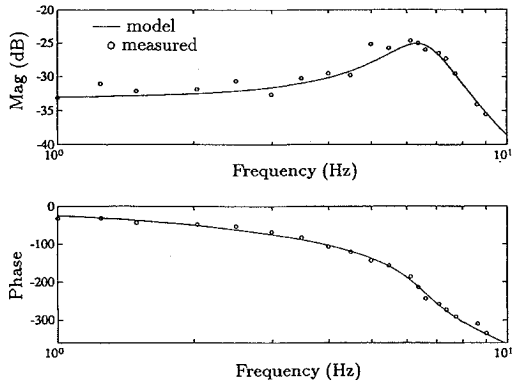

Fig. 11 System identification with sinusoidal forcing at near-optimal blowing rate.

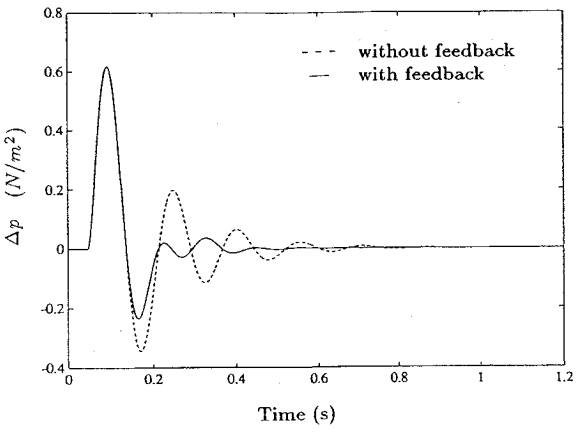

Fig. 12 Theoretical system response to an impulse.

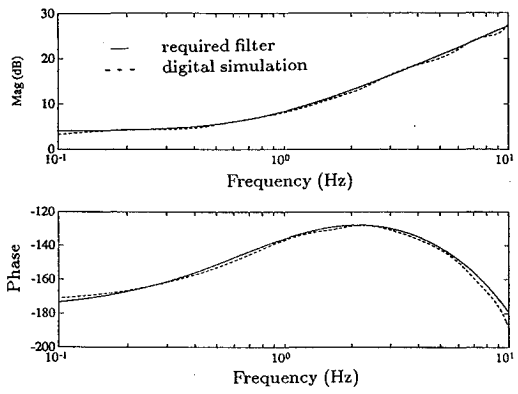

Fig. 13 Digital filter response.

The result is again found to match closely the measured data in Fig. 11.

The system without and with control can again be represented by replacing p_1 with Δp in Fig. 8. With the proportional control valve as feedback actuator, the magnitude drop at high frequencies is 40 dB/decade slower than that in the loudspeaker case. The phase drop, however, is faster due to the inherent time delay. We noted in Sec. V that we wish to make $|1 + G_1(s)G_2(s)H(s)|$ as large as possible to reduce the system sensitivity to noise. For absolute system stability, Nyquist criteria requires $|G_1(j\omega)G_2(j\omega)H(j\omega)|$ to be smaller than 1.0 as $\angle G_1(j\omega)G_2(j\omega)H(j\omega)$ reaches -180 deg. The rapid phase drop, therefore, limits the maximum of $|1 + G_1(s)G_2(s)H(s)|$ if simple constant gain feedback is used as in the loudspeaker case. As a result, a higher order filter is necessary. A second-order lead compensator $H(s)$ is designed by the loop-shaping approach.[16] The effect of the feedback is to cause the oscillatory system poles to migrate to more stable values. This is clear when we look at the theoretical system response to an impulse $v_f(s) = 1$ with and without $H(s)$ connected (Fig. 12).

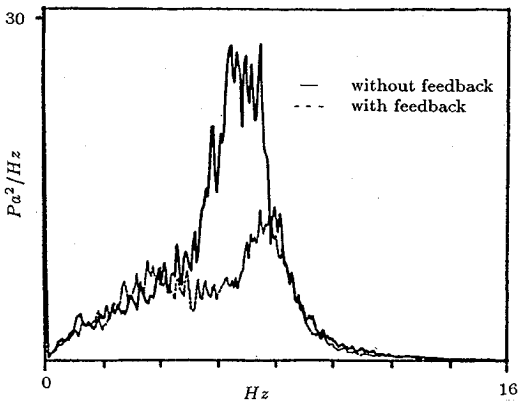

Fig. 14 Effect of active control with near-optimal mean blowing rate.

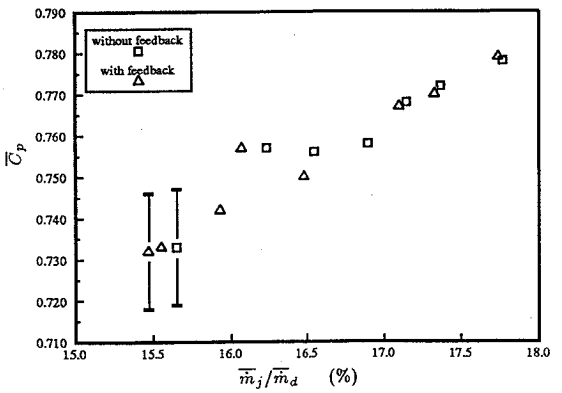

Fig. 15 Effect of feedback on pressure recovery.

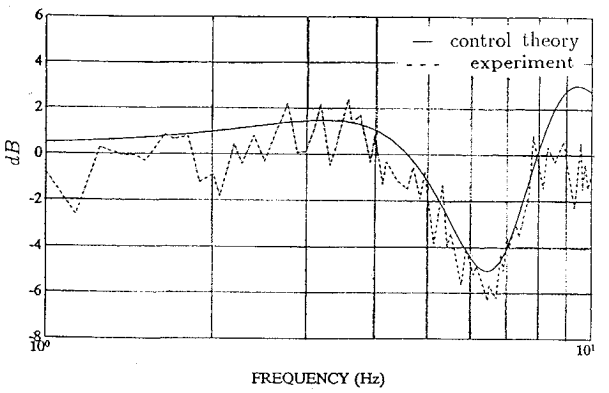

Fig. 16 Comparison of measured attenuation with theory, $\bar{m}_j/\bar{m}_d = 17\%$.

With bilinear transformation,[17] the equivalence of $H(s)$ in the z plane is found and implemented digitally at 200 Hz using the cascade method.[18] Δp signal from the pressure transducer is collected by the Microlink data logger modules PGA16 and BA12D. This is then processed according to the difference equation described by $H(z)$ in an Apricot Qi386 computer. The subsequent digital-to-analog (D/A) conversion is realized by the Microlink zero-order sample-and-hold[18] module 12DA. The required and digitally simulated lead compensator response $H(j\omega)$ are seen in Fig. 13 to agree well with each other.

The feedback system is found to be able to step down diffuser unsteadiness for fixed $\bar{m}_j/\bar{m}_d$ within the test range of $\bar{m}_j/\bar{m}_d$ from 15.5% to 18.0%. In Fig. 14, the feedback is seen to reduce the peak unsteadiness by 6 dB and the total power by 38%. $\bar{C}_p$ is again found to be unaltered by the feedback as shown in Fig. 15. The theoretical attenuation for the unsteadiness in Δp, as discussed in Eq. (4), is quantified by $|1/[1 + G_1(j\omega)G_2(j\omega)H(j\omega)]|$ on the assumption that the source of disturbance is not modified by the control. This is again found to agree well with the measured attenuation in Fig. 16.

VII. Conclusions

Steady blowing with suitably spaced circular nozzles is demonstrated to be an effective means of increasing diffuser pressure recovery. The nozzles are better than the conventional annular jet because they have a much smaller optimal injection rate and a simpler construction. The data from circular nozzles extends Duggins, statement[5] that diffuser performance with steady blowing is primarily governed by the injected-to-diffuser momentum flux. We show that this is not only true for the annular jets of different heights investigated by Duggins, but also applies when the wall jets have quite different geometries. Axial blowing is also shown to be successful at improving the recovery in rectangular diffusers.

Two active control methods have been applied to reduce transitory stall unsteadiness. The level of attenuation obtained can be predicted by theory. The combination of steady and unsteady blowing gives both a good mean pressure recovery and reduced pressure oscillations.

Acknowledgments

This work was carried out while one of the authors (AHMK) was in receipt of the Leslie Wilson Scholarship from Magdalene College Cambridge, an ORS award from the Committee of Vice-Chancellors and Principals, and funding from the Cambridge University Engineering Department and the Cambridge University Board of Graduate Studies. K. Glover's help in choosing the feedback filter in Sec. VII is gratefully acknowledged.

References

[1]Fox, R. W., and Kline, S. J., "Flow Regime Data and Design Methods for Curved Subsonic Diffusers," *Journal of Basic Engineering*, Vol. 84, 1962, pp. 303–312.

[2]Kline, S. J., "On the Nature of Stall," *Journal of Basic Engineering*, Sept. 1959, pp. 305–320.

[3]Gad-el-Hak, M., and Bushnell, D. M., "Separation Control: Review," *Journal of Fluids Engineering*, Vol. 113, 1991, pp. 5–30.

[4]Nicoll, W. B., and Ramaprian, B. R., "Performance of Conical Diffusers with Annular Injection at Inlet," *Journal of Basic Engineering*, Vol. 192, No. 4, 1970, pp. 827–835.

[5]Duggins, R. K., "Research Note: Conical Diffusers with Annular Injection," *Journal of Mechanical Engineering Science*, Vol. 17, 1975, pp. 237–239.

[6]Duggins, R. K., Lampard, D., and Sanders, A. T., "Further Investigation of Conical Diffusers with Annular Injection," *Journal of Mechanical Engineering Science*, Vol. 20, No. 1, 1978, pp. 58–65.

[7]Fiedler, R. A., and Gessner, F. B., "Influence of Tangential Fluid Injection on the Performance of Two-Dimensional Diffusers," *Journal of Basic Engineering*, Vol. 94D, 1972, p. 666.

[8]Kwong, A. H. M., and Dowling, A. P., "Unsteady Flow in Diffusers," *Journal of Fluids Engineering*, to be published.

[9]Smith, C. R., "Transitory Stall Time-Scales for Plane-Wall Air Diffusers," *Journal of Fluids Engineering*, Vol. 101, 1979, pp. 133–135.

[10]Putnam, A. A., *Combustion-driven Oscillations in Industry*, 1971, Elsevier.

[11]Ffowcs Williams, J. E., "Anti-Sound – Review Lecture," *Proceedings of the Royal Society of London*, Ser. A, Vol. 395, 1984, pp. 63–88.

[12]Nelson, P. A., and Elliott, S. J., *Active Control of Sound*, Academic Press, London, 1992.

[13]McDonald, A. T., and Fox, R. W., "An Experimental Investigation of Incompressible Flow in Conical Diffusers," *International Journal of Mechanical Science*, Pergamon Press Ltd. Vol. 8, 1966, pp. 125–139.

[14]Tijdeman, H., "On the Propagation of Sound Waves in Cylindrical Tubes," *Journal of Sound and Vibration*, Vol. 39, 1975, pp. 1–33.

[15]Anon., *Measurement of Fluid Flow in Closed Conduits*, BS1042, Bristish Standard Institution, 1980.

[16]McFarland, D. C., and Glover, K., "Robust Controller Design using Normalised Coprime Factor Plant Descriptions," *Lecture Notes in Control and Information Sciences*, Springer Verlag, Vol. 138, 1989.

[17]Franklin, G. F., and Powell, J. D., *Digital Control of Dynamic Systems*, Addison-Wesley, Reading, MA.

[18]Leigh, J. R., *Applied Digital Control*, Prentice-Hall International, Englewood Cliffs, N.J.